ELSEVIER

PII: S0032-3861(97)00068-2

Polymer Vol. 38 No. 21, pp. 5441–5446, 1997

0032-3861/97/$17.00 + 0.00

Effect of interface structure and amino groups on water splitting and rectification effects in bipolar membranes

Koji Shimizu and Akihiko Tanioka*
Department of Organic and Polymeric Materials, Tokyo Institute of Technology, Ookayama Meguro-ku, Tokyo 152, Japan
(Received 25 July 1996; revised 24 September 1996)

Bipolar membranes consist of a layered structure involving a cation selective membrane joined to an anion selective membrane. This is of practical interest in a new process for the commercial production of acids and bases. In this study, the mechanism of water splitting and the characteristics of the bipolar membranes were examined. It was suggested that water splitting occurred due to the second Wien effect in the intermediate region, because the potential drop was very large. If amines exist in the intermediate region, the water splitting is accelerated, because protonation and deprotonation reactions occur between H_2O and the amines. Current–voltage characteristics were correlated with water splitting effects. The efficiency of water splitting was increased by controlling the positions of the amino groups in the anion-selective polymer.

(Keywords: bipolar membrane; water splitting; membrane interface)

INTRODUCTION

The bipolar membrane is a layered structure involving a cation selective membrane joined to an anion selective membrane. It is well known that rectification is observed in current and voltage properties and water splitting occurs at the boundary between the anion and cation layers[1–3]. The water splitting mechanism has been discussed for a long time. Mafé and coworkers explained water splitting using the Donnan effect and the Nernst–Planck equation; water molecules dissociate into cations (H^+) and anions (OH^-) in accordance with the second Wien effect[4,5]. The efficiency of the water splitting is explained as a function of the dielectric constant in the boundary surface. On the other hand, Simons suggested that water splitting was caused by the chemical reaction of binary or ternary amino groups with water molecules[6–10].

In a previous paper, the effect of the polymer component and structure on membrane potential, rectification and water splitting in bipolar membranes was discussed[11]. The results of water splitting and rectification investigations showed that there was a good relationship between pH change in the cell and the current–voltage curve under reverse bias conditions, where the voltage was applied and the current flowed from positive to negative layers. Although it has been pointed out that the state of the intermediate boundary region is also responsible for water splitting, the results indicate that the chemical composition of the anion exchange layer plays an important role.

In this study, various kinds of bipolar membranes with different boundary structures consisting of a solution phase and binary, ternary and quaternary amines were prepared. Measurement of pH change under a constant applied voltage, and a current–voltage curve under reverse bias conditions were used to examine the mechanism of water splitting in bipolar membranes. If it is shown that the thickness or chemical composition of the boundary region is correlated with the current–voltage curve and pH change, it will be possible to provide a clear view of the water splitting mechanism.

EXPERIMENTAL

Samples

Two types of membranes, a hydrocarbon-type and a sandwich-type, were prepared.

Hydrocarbon-type membrane. For the preparation of the anion exchange layer, polyamine was added to a mixed solution of styrene and chloromethylstyrene in dimethylformamide (DMF) as a crosslinking agent. The solution was stirred for 1 min and cast on a glass plate surrounded by a rectangular frame (13 cm × 10 cm) of thickness about 1 mm. By drying at 125°C for 10 min, an anion exchange layer was obtained. Subsequently, a DMF solution of sulfonated poly(butadiene-*co*-styrene) rubber (Asahi Chemicals) was cast on the anion exchange layer surrounded by the rectangular frame to dry, at 125°C for 6 min in the air for the preparation of the cation exchange layer. The glass plate was spontaneously cooled down to room temperature and soaked in 0.1 mol dm^{-3} aqueous solution of potassium chloride to peel off the membrane. At this time, we prepared two types of membrane by selecting different kinds of

* To whom correspondence should be addressed

Table 1 Thickness and charge density of membranes

Membrane	Cation exchange layer		Anion exchange layer	
	Thickness (μm)	Charge density (mol dm^{-3})	Thickness (μm)	Charge density (mol dm^{-3})
H-1	35	0.92	75	0.65
H-2	35	0.92	75	0.65
K-172 (Asahi Chemicals)	120	0.68		
A-172 (Asahi Chemicals)			140	0.58

polyamines. The mixture of *N,N,N′,N′*-tetramethyl-1,6-diaminohexane (Asahi Chemicals) and *N,N*-dimethyl-1,3-propanediamine (Asahi Chemicals) (1 mol/3 mol) was used for the sample called H-1, and *N,N,N′,N′*-tetramethyl-1,6-diaminohexane was used for the sample called H-2.

Sandwich-type membrane. The anion exchange membrane containing a quaternary amine group (A-172, Asahi Chemicals) and the cation exchange membrane containing a sulfonic acid group (K-172, Asahi Chemicals) were superimposed. The main polymer composition of both membranes is similar to that of the hydrocarbon-type membrane cited above. However, this membrane is supported by woven cloth in order to prevent further water swelling. The intermediate region is presumed to be a very thin water layer. The thickness and fixed charge density of each membrane are shown in *Table 1*.

Measurement of current–voltage curves under reverse bias conditions

The current–voltage curves under reverse bias conditions across the membrane were measured with the feeler method (4-point method)[11,12]. The membrane (cross-sectional area $A = 7\,cm^2$) was placed between two electrodialytic half cells with 0.1 mol dm^{-3} aqueous solution of potassium chloride, and two Pt-black electrode wires (diameter $\phi = 0.3$ mm) were laid on both surfaces of the membrane. The current was introduced through two Pt-black electrode plates of cross-sectional area $A = 7\,cm^2$. The applied voltage (V) was measured by a voltage meter (TOA, PM-16A) and the current (I) by a picoammeter (TOA AM-271A). I–V curves were determined between measuring current and the applied voltage across the membrane with the plates and wires, respectively, after 5 min from the start of the measurement. Under reverse bias conditions current and voltage are promised to be the negative values which appear in the third quadrant. However in this study measured current and voltage are multiplied by -1 in order to give in the first quadrant, as shown in *Figures 1–5*.

Electrodialysis measurements

The measurements of pH change caused by water splitting were carried out using a laboratory-scale cell designed for the production of acids and bases[11]. The cell was composed of four compartments as shown in *Figure 6*. The two outside compartments (L_2, R_2) were separated by a cation or anion exchange membrane, where the effective area $A_m = 8\,cm^2$, respectively, and Pt-black electrodes were installed at the opposite sides of the ion-exchange membranes. In these two compartments, circulation of a 0.1 mol dm^{-3} aqueous solution of

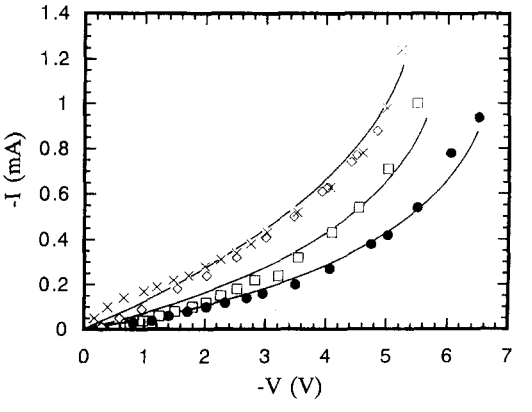

Figure 1 I–V characteristics of H-1 membrane at various concentrations of KCl aqueous solution: 0.025 mol dm^{-3} (●), 0.05 mol dm^{-3} (□), 0.075 mol dm^{-3} (◇) and 0.1 mol dm^{-3} (×). Solid lines show the calculated results by equation (3)

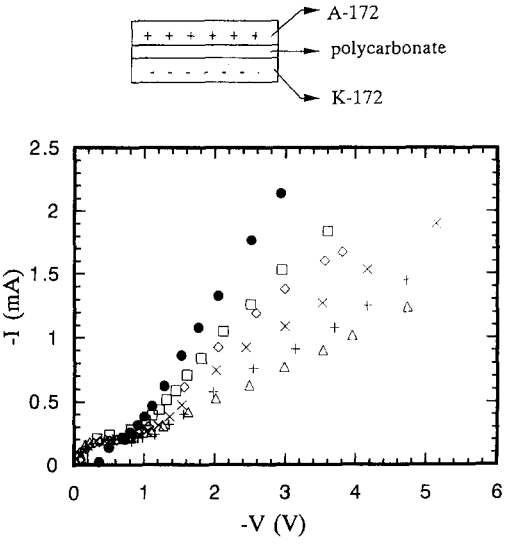

Figure 2 I–V characteristics of sandwich-type membrane as a function of thickness in the boundary region, where the thickness is enlarged by porous polycarbonate membranes (Nuclepore) of different thicknesses: 0 μm (●), 10 μm (□), 20 μm (◇), 30 μm (×), 40 μm (+) and 50 μm (△)

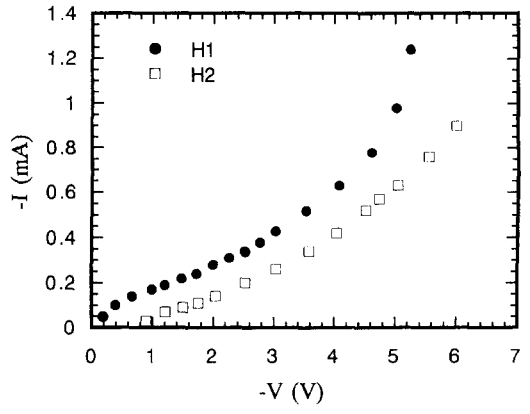

Figure 3 I–V characteristics of H-1 (●) and H-2 (□) membranes

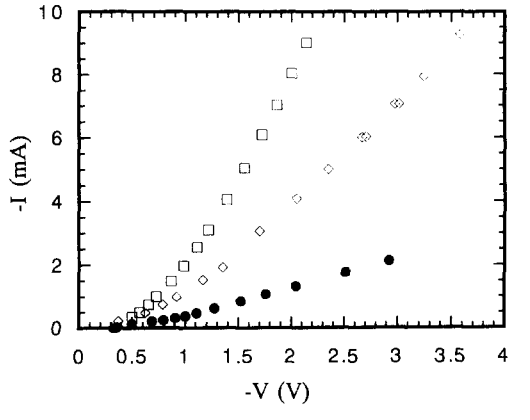

Figure 4 Comparison of I–V characteristics among sandwich-type membranes when various membranes were installed between K-172 and A-172, as the intermediate region. The anion exchange layer of H-1 (□), the anion exchange layer of H-2 (◇), and nothing (●)

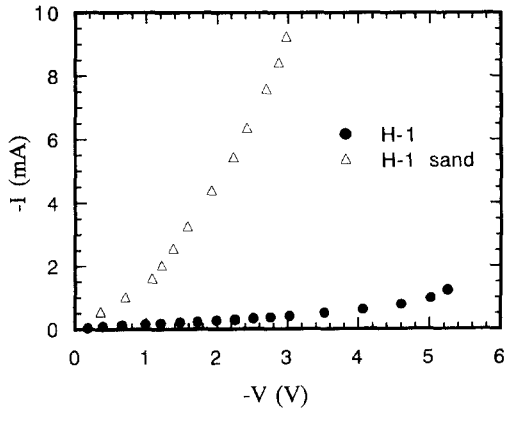

Figure 5 Comparison of I–V characteristics between H-1 and 'H-1 sand'. For sample 'H-1 sand', the cation and anion exchange layers were cast separately

potassium chloride was maintained. The two central compartments (L_1, R_1) were divided by the bipolar membrane ($A_m = 8\,cm^2$), 200 ml of 0.1 mol dm^{-3} KCl aqueous solution was circulated in each central compartment and the pH variation of each potassium chloride aqueous solution was measured in each outside container using pH meters (HM-20E, TOA). The applied voltage was provided from an electrode in L_2 to one in R_2, by a direct current (d.c.) source (Kikusui PAB18-1A) for 1 h. The applied voltage was varied from 2 to 10 V. At this time, the anion exchange layer of the bipolar membrane faced toward the anode and the cation exchange layer toward the cathode, and the distance between anode and cathode was 2.5 cm. N_2 gas was introduced into each compartment of ion-exchanged water, to avoid acidification by CO_2 absorption, for 1 h before, and during the experiment.

RESULTS AND DISCUSSION

Mechanism of water splitting

Figure 1 shows the current–voltage curves with sample H-1 at different KCl concentrations under reverse bias conditions. As described previously, the measured current and voltage are multipled by −1 in order to give in the first quadrant. Current is obtained in all situations, although those phenomena are not observed with a p-n junction of a semiconductor, so the current can be explained by the flow of H^+ and OH^- ions generated by water splitting. Electrolysis of water is one of the factors which generate water splitting. However, the observed electric currents under reverse bias in *Figure 1* are so high that water splitting cannot be explained by only electrolysis. Therefore, this is a specific characteristic of the bipolar membrane.

One possible explanation was suggested by Wien and Schile[13]. They pointed out that the ion mobility increases with increasing electric field in weakly dissociated electrolytes. This effect has been called the second Wien effect, and the theory was developed by Onsager[14] and Harned and Owen[15]. Water is a weakly dissociated electrolyte; therefore this theory can be applied to bipolar membranes[5]. A high electric field is generated at the space charge region with a p-n junction. Because the structure of the bipolar membrane resembles that of a semiconductor, such a high electric field may be produced. *Figure 2* shows the current–voltage characteristics with a sandwich type membrane on varying the thickness of the intermediate region between the anion and the cation exchange layers by inserting a stack of porous polycarbonate membranes at 0.1 mol dm^{-3} KCl aqueous solution. Experimental results indicate that the electric current decreases according to the increase in the intermediate region thickness. Considering the structure of the porous polycarbonate (pore size $\phi = 5.0\,\mu m$), the decrease in the electric field magnitude can be explained. Mafé and coworkers reported the ion flux in bipolar membranes under a reverse bias[4,5]. They used the second Wien effect to quantify the efficiencies of water splitting using Onsager's theory[14]. In their papers, the dissociation constant of water, k_d, is written in the following form:

$$\frac{k_d}{k_d^0} \approx \left(\frac{2}{\pi}\right)^{1/2} (8b)^{-3/4} \exp[(8b)^{1/2}] \quad (1)$$

$$b \equiv \frac{0.096}{\epsilon_r T^2} E \quad (2)$$

where k_d^0 is the steady state water dissociation constant, E is the electric field and ϵ_r is the relative electric permittivity of the intermediate region in the membrane. The bias voltage dependence of the current using the

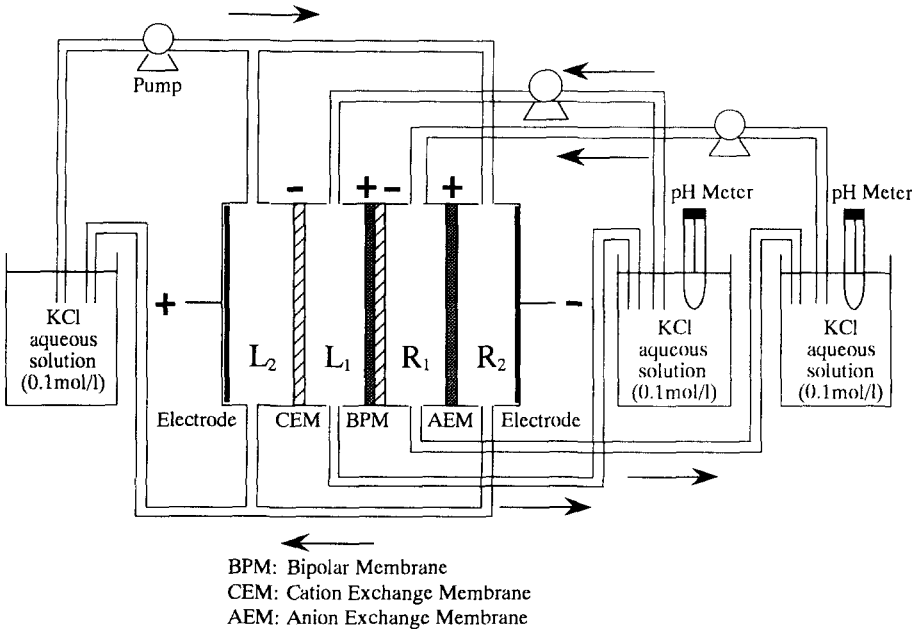

Figure 6 Schematic diagram of the electrodialysis cell arrangement used for measuring water splitting properties

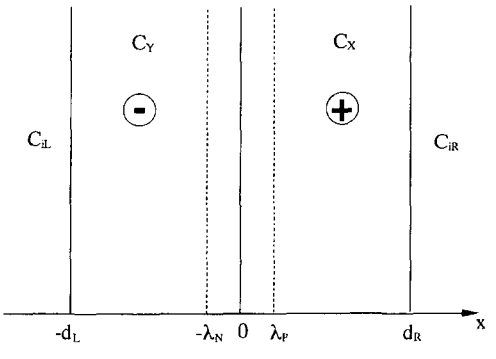

Figure 7 Schematic diagram of the model of the bipolar membrane. The region from $-\lambda_N$ to λ_P corresponds to the space charge layer

space charge model shown in *Figure 7* can be written in the form:

$$I = F\left(\frac{D_{1P}}{d_R}\bar{C}_{1P}(d_R) + \frac{D_{2N}}{d_L}\bar{C}_{2N}(-d_L)\right)\left[\exp\left(\frac{FV}{RT}\right) - 1\right] + F[D_{3P}\beta_P\bar{C}_{3P}(d_R)\coth(\beta_P d_R) + D_{4N}\beta_N\bar{C}_{4N}(-d_L)\coth(\beta_N d_L)]\left[\exp\left(\frac{FV}{RT}\right) - 1\right] - Fk_dC_W\lambda \quad (3)$$

$$\beta_N = \sqrt{\frac{k_r^0\bar{C}_{3N}(-d_L)}{D_{4N}}} \quad (4)$$

$$\beta_P = \sqrt{\frac{k_r^0\bar{C}_{4P}(d_R)}{D_{3P}}} \quad (5)$$

$$\lambda \equiv \lambda_N + \lambda_P = \sqrt{\frac{-2\epsilon_r\epsilon_0}{F}V\frac{C_X + C_Y}{C_XC_Y}} \quad (6)$$

where D_{ik} stands for the diffusion coefficient of species 'i' in the 'k' region. $\bar{C}$ is the concentration of ions in the membrane. C_X and C_Y are charge densities in the anion and cation exchange layers. We tried to fit equation (3) to our experimental results. The ϵ_r value in the membrane was used as the fitting parameter because it could not be determined. Other parameters took the values: $D_{1P} = D_{2N} = 10^{-9}$ ($m^2\,s^{-1}$) and $D_{3P} = D_{4N} = 10^{-8}$ ($m^2\,s^{-1}$). In *Figure 2*, solid lines show the theoretical curves using equation (3). Curve fittings were theoretically successful when the dielectric constants were given the values shown in *Table 2*, which were between those of water (*ca* 78) and dried polymer (*ca* 10). Unfortunately, the dielectric constant of the hydrated membrane cannot be determined exactly. The permittivity of the aqueous polymer gel film is supposed to be between those of water and the polymer, using Bruggeman's equation[16], and the measured values of the aqueous poly(vinyl alcohol) gel film were between 30 and 100[17]. Therefore, the results in *Table 2* are reasonable. If, however, the applied voltage was 0.3 V where the water splitting started, the electric field calculated by equation (3) in the space charge region was 2.06×10^8 ($V\,m^{-1}$), and did not attain the order of 10^9 ($V\,m^{-1}$) at which the second Wien effect should occur, even if we use the calculated values in *Table 2* for the dielectric constant. This is due to ignoring the effect of the membrane potential, which is composed of Donnan and diffusion potentials. In our calculation, we use zero in the membrane potentials. However, the Donnan potential is actually not zero in bipolar membranes, as shown in the previous paper[11]. Especially, at the surface facing the intermediate region, a relatively high Donnan potential is presumed to be generated under the bias condition. When a potential of 1 V is

Table 2 Dielectric constant of the membrane calculated by equation (3)

C_S ($mol\,dm^{-3}$)	ϵ_r
0.025	52.2
0.050	51.3
0.075	45.4
0.100	45.3

applied, the concentration at the surface relative to the space charge region is $< 10^{-7}$ (mol dm^{-3}) and the Donnan potential reaches about 1 V[11]. The width of the space charge region is supposed to be equal to about 10^{-9} m. If the potential and the width in the space charge region cited above are considered, the value of E in equation (2) becomes the optimum magnitude to cause the second Wien effect.

Secondly, current–voltage curves under reverse bias conditions for H-1 and H-2 at 0.1 mol dm^{-3} KCl solution are shown in *Figure 3*. H-1 is composed of secondary, tertiary and quaternary amino groups, and H-2 only of a quaternary group. Considering that the difference in both samples is only the amino groups in the anion exchange layer, such a difference cannot be explained by only the second Wien effect. Simons reported that a proton transfer reaction occurs in the anion exchange layer[8,9].

$$\begin{aligned} B + H_2O &\rightarrow BH^+ + OH^- \\ BH^+ + H_2O &\rightarrow B + H_3O^+ \end{aligned} \qquad (7)$$

'B' represents a neutral base group such as RNH_2 or R_2NH. These reactions do not occur around quaternary amino groups, because there is no space for the proton to unite with the amino group. *Figure 4* shows current–voltage curves with sandwich-type membranes in which various materials were inserted between K-172 and A-172. When an anion exchange layer of H-1 or H-2 was inserted, the efficiency of water splitting increased. Especially, the highest efficiency was observed for the sample in which the anion exchange layer of H-1 was inserted. This result agrees with the chemical reaction suggested by Simons[9,10]. Though the anion exchange layer of H-2 has only quaternary amino groups, the efficiency of water splitting increased. This can be explained by the existence of uncrosslinked tertiary amines.

There are two reasons that the proton transfer reaction accelerates the water splitting at bipolar membranes. The first is the influence of the electric field, which causes the orientation of the water molecules to take an optimum position for the reaction with an amino group. The second is the influence of the counter ion on the protonated amino group in the space charge region. The concentration of the counter ion is very low in this region, because it is extracted from the membrane to a cathode. Therefore, protonated amino groups without a counter ion simultaneously react with water, as shown in equation (7).

It has been said that both the second Wien effect and the proton transfer reaction cause water splitting. Especially, the proton transfer reaction in the space charge region is a unique mechanism, which contributes to the higher efficiency of water splitting at bipolar membranes. However, there are problems concerned with evaluating membrane properties only by current–voltage characteristics. *Figure 5* shows the current–voltage characteristics with H-1 and 'H-1 sand', which is a sandwich-type membrane of H-1 (the anion and cation exchange layers were cast separately and laid one on top of the other). Though they are made of the same matrices, and have the same charge densities and thicknesses, the observed currents are not the same at all. Thus, other methods have to be used to evaluate the efficiencies.

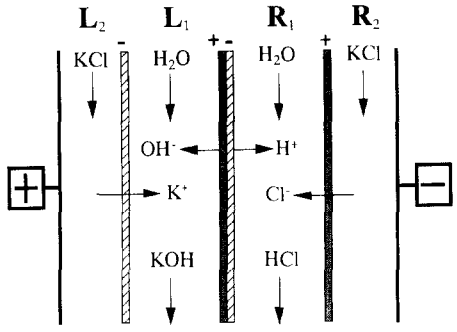

Figure 8 Process for the production of acid and base

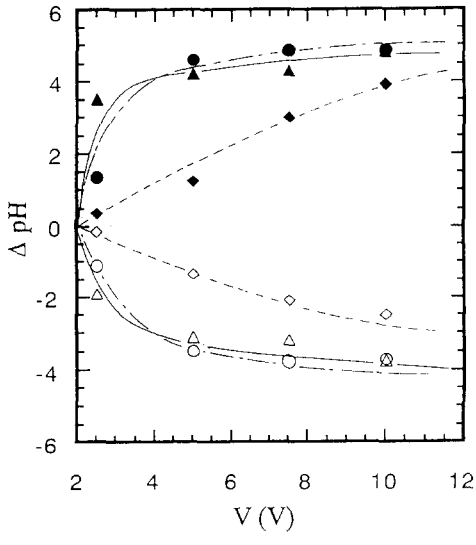

Figure 9 Bias voltage dependence of pH change: (△ and ▲) for H-1, (◇ and ◆) for H-2, (○ and ●) for H-1 sand. Open and closed symbols show the pH change at the cation exchange layer side and the anion exchange layer side, respectively

Relation between current–voltage characteristics and pH changes under constant applied voltage[11]

A schematic drawing of the acid and base purification is shown in *Figure 8*. If the direct voltage is applied in the proper direction, which is from the cation exchange to the anion exchange layer, H_2O diffusing into the intermediate boundary region is dissociated into H^+ and OH^- ions under the electric field. The K^+ and Cl^- ions permeate through the monopolar cation and monopolar anion exchange membranes from the side compartments (R_2, L_2) to the two central compartments (R_1, L_1), respectively, where ion-exchanged water is circulating independently. Thus, acid in R_1 and base in L_1, respectively, are produced. The results of electrodialysis with H-1 and H-2 are shown in *Figure 9*. The pH change of the H-1 membrane is larger than that of H-2, and this is in good accord with the current–voltage characteristics. *Figure 9* also shows the results for 'H-1 sand'. Though the current–voltage characteristics are absolutely different from that of H-1, the pH change is almost the same. This can be explained by assuming that the current which is observed in 'H-1 sand' is caused by the flow of ions other than H^+ and OH^-. It is assumed that a solution region exists between the anion exchange layer and a cation exchange layer in a sandwich-type membrane, because those two layers were only superimposed on each other. Therefore, K^+ and Cl^- ions in

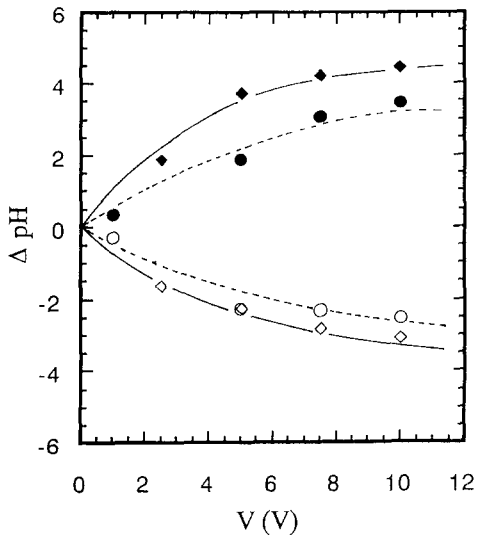

Figure 10 Bias voltage dependence of the pH change when poly(oxyethylene alkylamine) was adsorbed between K-172 and A-172: (◇ and ◆) for adsorbed sample; (○ and ●) for non-adsorbed sample. Open and closed symbols show the pH change at the cation exchange layer side and the anion exchange layer side, respectively

this region may influence the current–voltage characteristics and make it difficult to quantify the generated H^+ and OH^-.

Finally, we tried to control the arrangement of amino groups in the anion exchange layer. Polyoxyethylene-alkylamine (Kao Chemicals Co.) was absorbed on one side of A-172 to form a monomolecular layer. Then K-172 was laid on top of that layer. As a result of this arrangement, the anion exchange layer has tertiary amino groups in the space region where the proton transfer reaction occurs, and quaternary amino groups, which are excellent for permselectivity, in the other space. The results of the water splitting experiments with this sample are shown in *Figure 10*. The pH change of the adsorbed sample is larger than that of the unadsorbed one, where the cation and anion exchange layers consist of K-172 and A-172 membranes. Therefore, if it is possible to form the membrane in one united body, a higher performance bipolar membrane can be obtained.

CONCLUSIONS

In this study, it was proved that water splitting occurred due to both the second Wien effect at the intermediate region and the protonation and deprotonation reactions between H_2O and amines in the anion exchange layer. The efficiency of water splitting was increased by controlling the positions of the amino groups in the anion selective layer.

ACKNOWLEDGEMENT

We are most grateful to Mr Hamada and Mr Noaki of Asahi Chemical Co., Ltd, for providing us with the samples and for helpful suggestions.

REFERENCES

1. Bassignana, I. C. and Reiss, H., *J. Membr. Sci.*, 1983, **15**, 27.
2. Mauro, A., *Biophys. J.*, 1962, **2**, 179.
3. Coster, H. G. L., *Biophys. J.*, 1965, **5**, 669.
4. Ramirez, P., Manzanares, J. A. and Mafé, S., *Ber. Bunsenges. Phys. Chem.*, 1991, **95**, 499.
5. Mafé S., Manzanares, J. A. and Ramírez, P., *Phys. Rev. A*, 1990, **42**, 6245.
6. Ramirez, P., Rapp, H. J., Reichle, S., Strathmann, H. and Mafé, S., *J. Appl. Phys.*, 1992, **72**, 259.
7. Ramírez, P., Rapp, H.-J., Mafé, S. and Bauer, B., *J. Electroanalytical Chem.*, 1994, **375**, 101.
8. Simons, R., *Desalination*, 1979, **28**, 41.
9. Simons, R., *Nature, Lond.*, 1979, **280**, 824.
10. Simons, R., and Khanarian, G., *J. Membr. Biol.*, 1978, **38**, 11.
11. Tanioka, A., Shimizu, K., Miyasaka, K., Zimmer, H. J. and Minoura, N., *Polymer*, 1996, **37**, 1883.
12. Yokoyama, M., Tanioka A. and Miyasaka K., *J. Membr. Sci.*, 1989, **43**, 165.
13. Wien, M., and Schile, J., *Phys. Z.*, 1931, **32**, 545.
14. Onsager, L., *J. Chem. Phys.*, 1934, **2**, 599.
15. Harned, H. S. and Owen, B. B., *The Physical Chemistry of Electrolyte Solutions*, 3rd edn. Reinhold, 1958.
16. Bruggeman, D. A. G., *Ann. Physik*, 1935, **24**, 636.
17. Okumura, J., Taguchi M., Tanioka A., and Miyasaka K., *Polymer Preprints, Japan*, 1991, **40**, 2134.